

THERMAL SHOCK IN ANODES FOR THE ELECTROLYTIC PRODUCTION OF ALUMINIUM

E. Kummer  
 Helbling Technik AG, Neumattstrasse 30  
 CH - 5000 Aarau, Switzerland  
 Dr. W. Schmidt-Hatting  
 Aluminium & Chemie Rotterdam B.V.  
 Oude Maasweg 80  
 NL-3197 KJ Botlek-Rotterdam, The Netherlands

Abstract

There are many publications describing the resistance to cracks caused by thermal shock in ceramic bodies by using quality figures. In *Light Metals 1988* these figures were applied to anodes for the aluminium industry. Such quality figures allow a simple and fast appraisal of an anode's tendency to thermal shock. The application of these quality figures in practice has shown, however, that a modification of the definition of the quality figure thermal shock is advisable. The mechanical stresses, which occur when a heat wave penetrates the cold anodes after they are set in the hot electrolyte, were calculated three-dimensionally. The results confirm the validity of the already mentioned quality figures on the one hand and correspond very well to the shape of cracks in anodes observed in practice. The influence of the conditions under which the anodes are set and of the properties of the anodes on the mechanical stresses which arise, is reported on.

INTRODUCTION

In numerous publications quality figures - mostly for ceramic bodies - have been published [1, 2,3,4], which describe the resistance to the occurrence or spreading of a crack due to thermal shock. In *Light Metals 1988* such quality figures were applied to prebaked anodes [5]. The experience which has been gained in the meantime makes it seem advisable to modify the formula of the quality figure in order to attain a better agreement with practice. Furthermore in the following a report is given on three-dimensional computer calculations for determining the mechanical stresses, which occur when a cold anode is set into the hot electrolyte.

EXPERIENCE WITH THE QUALITY FIGURE THERMAL SHOCK

Change in the Definition of the Quality Figure

The quality figure indicated in 1988 was as follows [5]:

$$TSFR(2) = \frac{(\sigma_B/\sigma_{B0}) * (\lambda/\lambda_0)}{(\gamma/\gamma_0) * (E/E_0) * (\alpha/\alpha_0)} \quad (1)$$

Significances in equation 1:

- $\sigma_B$  bending strength, in N/m<sup>2</sup>
- $\lambda$  thermal conductivity, in W/mK
- $\gamma$  apparent density, in kg/dm<sup>3</sup>
- $E$  Young's modulus, in N/m<sup>2</sup>
- $\alpha$  thermal expansion coefficient, in 1/K

Index "zero" characterizes the standard values of the crack-free populations. The standard values depend on the raw materials used and the recipes and are, therefore, not absolute values.

Taking this into account, the following guide values can be indicated for the standard values:

- $\sigma_{B0} = 140 \cdot 10^5$  N/m<sup>2</sup> for vibrated anodes
- $= 125 \cdot 10^5$  N/m<sup>2</sup> for pressed anodes
- $\lambda_0 = 2.8$  W/mK
- $\gamma_0 = 1.6$  kg/dm<sup>3</sup>
- $E_0 = 7000 \cdot 10^6$  N/m<sup>2</sup>
- $\alpha_0 = 4.0 \cdot 10^{-6}$  1/K

Since the bending strength is representative for the tensile strength, the latter being difficult to measure on the anode, it was to be expected that high values for  $\sigma_B$  are equivalent to high resistance to thermal shock.

Practice has shown, however, that high values for  $\sigma_B$  indicate a marked brittleness of the anodes and with that a high tendency to thermal shock cracks. For vibrated anodes this range is above  $140 \cdot 10^5$  N/m<sup>2</sup> and for pressed anodes above  $125 \cdot 10^5$  N/m<sup>2</sup>. For that reason equation 1 is changed to:

$$Q_{TS} = TSFR(2) = \frac{(\lambda/\lambda_0)}{(\sigma_B/\sigma_{B0}) * (\gamma/\gamma_0) * (E/E_0) * (\alpha/\alpha_0)} \quad (2)$$

Such a change was announced orally in the presentation of the publication [5] in 1988.

For equation 2 the following limitations apply:

- $(\lambda/\lambda_0) \leq 1$
- $(\alpha/\alpha_0) \geq 1$
- $(E/E_0) \geq 1$
- $(\gamma/\gamma_0) \geq 1$
- $(\sigma_B/\sigma_{B0}) \geq 1$

With that  $Q_{TS}$  can only be "1" or smaller than "1". If  $Q_{TS}$  falls below 0.9, there is the risk of thermal shock.

Correlation Test on Anode Properties

In anode production it must now be attempted to obtain such physical properties of the anodes in accordance with equation 2, which guarantee that one remains safely within the crackfree area. In order to find out what properties have to be given special attention, the properties according to equation 2 were examined for reciprocal correlation. The result can be seen from Table 1.

In Table 1 it can be clearly recognized that  $\alpha$  is not correlated with any other factor. It can, therefore, in a first approach, not be influenced by anode production parameters. Tests conducted with various coke mixtures in the dry aggregate of the anodes have shown that  $\alpha$  is to be attributed to the properties of the coke.

Correlation between	Correlation Coefficient
$\sigma_B$ and E	0.76
$\gamma$ and E	0.81
$\lambda$ and E	0.70
$\alpha$ and E	0.20
$\gamma$ and $\sigma_B$	0.49
$\lambda$ and $\sigma_B$	0.26
$\alpha$ and $\sigma_B$	0.18
$\gamma$ and $\lambda$	0.66
$\gamma$ and $\alpha$	0.22
$\lambda$ and $\alpha$	0.18

Table 1: Correlations between physical properties of prebaked anodes

The thermal expansion coefficient of anodes can, therefore, primarily be controlled solely by a suitable choice of coke.

Taking the correlations shown into consideration, equation 2 can be approximated by:

$$\overline{Q_{TS}} = \frac{1}{\sigma_B^2 \cdot \alpha} \quad (3)$$

Equation 3 serves only to estimate the influence of the factors and may not be used to calculate the risk of thermal shock cracks; for that only equation 2 should be used.

With that the limit value of  $\sigma_B$  becomes more important besides  $\alpha$ . Furthermore, equation 3 indicates that the spreading of cracks can be more important than their actual occurrence [5].

CALCULATION OF THE MECHANICAL TENSIONS

Introduction

The three-dimensional calculation with finite elements of the mechanical stresses as function of place and time in an anode is no longer a problem mathematically today, if the border conditions when a cold anode is dipped into the hot electrolyte have

been established and all the material values of the anode are known.

The necessary material values for the calculations are the same as used in equation 2. However, they must be known as a function of the temperature. If one or more of them shows a dependency on the temperature, then one has a non-linear system, the equation systems of which can be solved incrementally, although as a result the computation times become considerably longer.

Another factor which is required is the heat transfer coefficient  $\beta$  between the liquid, hot and moved electrolyte and the cold anode. It has to be taken into account that first of all a solidified electrolyte crust forms around the cold anode, which then melts down as the anode becomes hotter.

There were no prospects of finding reliable values for all these factors in the literature. Anodes were equipped with distributed thermocouples, therefore, in order to measure the rise in temperature after the anode is set in the hot electrolyte as a function of locus and time and thus to be able to conclude the uncertain factors (mainly  $\beta$ ).

In addition the increase in the anode current has to be taken into account, for it represents a source of heat in the anode.

Temperature Measurements in the Anodes

In the anodes 15 temperature measuring points were distributed spatially in such a way as to allow the penetration of the heat wave at relevant points on the anode to be kept track of.

Parallel to that, the temperatures were calculated. The comparison calculation - measurements then supplied a value for the heat transfer coefficient electrolyte - anode of

$$\beta = 17.5 \text{ W/m}^2 \text{ K}$$

This value is very small for a moved liquid compared to other agents and can only be explained by the fact that a thin crust forms on the underside of the anode, which only completely melts hours after being set.

In the temperature calculations it was still assumed that the thermal conductivity changes as function of the temperature like the electrical conductivity. That means for example an increase of  $\lambda$  by 13% for a temperature rise of 200° C. This increase corresponds very well with other published data [6]. The comparison measurement - calculation then showed that the values for  $\lambda$  indicated in the literature are confirmed.

Physical Factors

Physical properties which were regarded as independent of the temperature, were taken into account as follows:

- specific heat:  $c_0 = 0.97 \text{ J/gK}$
- apparent density:  $\gamma = 1.571 \text{ kgC/dm}^3$
- Young's modulus:  $E = 6796 \cdot 10^6 \text{ N/m}^2$
- Thermal expansion coefficient:  $\alpha = 3.5 \cdot 10^{-6} \text{ 1/K}$
- Poisson's ratio:  $\mu = 0.2$

Anodic Current

For the anodic current it was assumed that it rises linearly with the time from zero to the anode nominal current after 18 hours and then remains constant.

Method of Calculation

The thermal and mechanical calculations of the carbon anodes were carried out with the finite element program TPS10 [7]. This program system was developed in Germany and allows extensive possibilities for application in the sectors of statics, dynamics and potential problems. Linear and nonlinear calculations are possible with time-dependent temperature and material characteristics, which are close to reality.

In order to achieve as fine an element distribution as possible, only a quarter of the anodes was included in the calculation in each case. That means that a symmetrical temperature distribution was taken as a premise as regards the two symmetry axes. This is probably in reality pretty well the case; in the first few minutes after setting the anode in the reduction pot, it probably is very accurate.

In the calculations the anode assembly is neglected because thermal shock cracks occur in the first few minutes. At this point of time, the steel parts cannot yet exert any force on the anode because it is still not hot.

Finite Element Models (FE Models)

The preparation of a finite element model for the carbon anode was very difficult because on the one hand the number of nodes was not allowed to be too high and on the other the distribution along the outside surfaces had to be relatively fine, because in these regions high temperature gradients occur at the start.

This was solved in such a way that an element type of the second degree was chosen i.e. an element is defined by the eight corner nodes and the twelve intermediate nodes (in the middle of the element edges). This gives a total of twenty nodes per element.

For all types of anodes an immersion depth in the electrolyte of 15 cm was set. Vertically the elements were arranged in seven layers in accordance with Figure 1. That gives a total of approx. 250 elements in an anode quarter with about 1400 nodes.

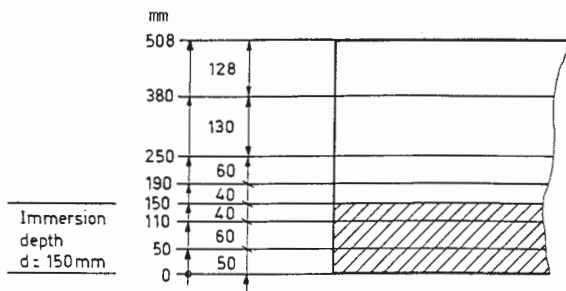


Figure 1: Layer distribution of the elements

Boundary Conditions

For the physical description of the computer model, on the one hand thermal boundary conditions are to be applied and on the other the mechanical boundary conditions are to be indicated, which are necessary for calculating the stresses. Naturally the fact has to be taken into account that only a quarter of the anode is calculated. The influence of the parts left out can be compensated with the boundary conditions.

With the indication of the heat transfer coefficient  $\beta$  and the ambient temperature, the boundary conditions on the outside surfaces are adequately defined. As bath temperature, 965° C was set. The ambient temperature at the upper part of the anode was assumed to be 800° C. The standard immersion depth into the bath was 150 mm.

In the symmetry planes no heat should flow for reasons of symmetry.

For the mechanical boundary conditions in the symmetry planes, the normal symmetry boundary conditions are to be entered i.e. the node shift normal to the sectional plane must be zero. In addition a further boundary condition in the third coordinate is necessary in order to prevent a rigid body motion.

Resulting Residual Stresses

After determining the temperature distribution as function of the time, the calculated temperatures on the nodes were taken and from that the deformation and the stresses in the carbon block were determined. Since the point of time of the maximum stresses which occur was unknown at first, the first twenty temperature increments were calculated, which altogether cover a period of approx. 25 minutes from the point of time of setting.

RESULTS

Relatively Small Anode

If one analyzes the computation results, the following can be ascertained:

- the place of maximum stress is in the proximity of the lower corners.
- the amount of maximum stress rises with increasing time and finally reaches a maximum. Subsequently it slowly drops again.
- The place of maximum stress seems to move away from the lower corner with increasing time.

Very informative is the stress curve as function of the time. Fig. 2 shows the curve for four nodes. Node 282 reaches the maximum value of the main tensile stress of  $\sigma = 1.93 \text{ N/mm}^2$  after 4.5 minutes.

Subsequently the curve slowly drops off. The stresses in the node 227 (same height as 282, but further in) reach the maximum after approx. 18 minutes with a maximum stress of  $2.45 \text{ N/mm}^2$ . The node 457 (60 mm above 257) reaches a maximum even later, and the maximum stress value is even slightly higher.



The direction of the main tensile stress in the lower corner of the anode runs fairly exactly in the space diagonal of the anode. If one determines the place of the maximum stress, then the form of the corner crack can be determined assuming that the crack forms exactly at the place of the maximum main tensile stress and continues outwards.

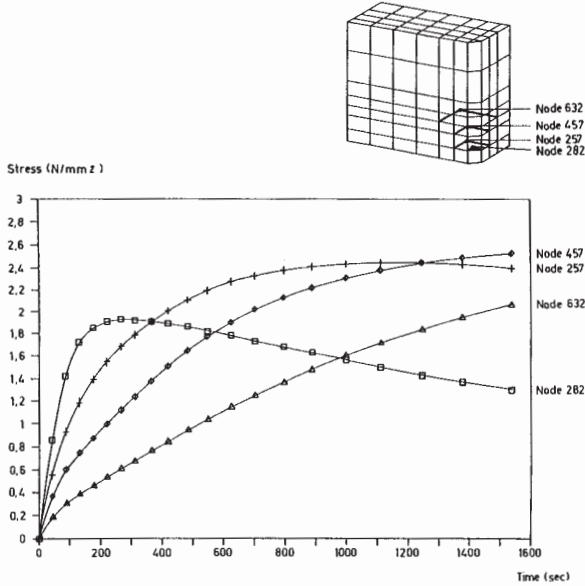


Fig. 2: Time curve of the main tensile stresses in the range of the lower anode corners

Fig. 3 shows the form of the crack on the outside surfaces. Since the stress curve at the place of maximum stress is very flat, the crack can shift a few centimetres depending on where the weakest point in the anode is or where there already was a fine haircrack.

The results of the stress calculations as a consequence of the temperature shock when setting can be interpreted as follows:

- Shortly after the anode is set, zones of tensile stresses form parallel to the lower edges. These zones are initially about 50 mm within the two side areas and at about 50 mm height.
- In the corner area the two tensile zones from the long and short side meet, with the result that also the tensile stresses superimpose each other.

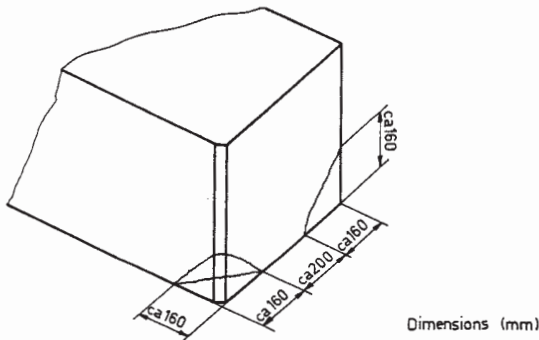


Fig. 3: Crack lines of a corner crack (determined mathematically)

- Approx. 4.5 minutes after setting, a first stress maximum forms in the corner area. Subsequently the stress at this place slowly declines again.
- With increasing time the place of the stress maximum moves further in and further up. Also the amount of the stress maxima increases at first.
- The amount of the tensile stresses remains at all times under the bending strength. It reaches only about 20 - 25 % of the strength of the anode.

With this result it is also clear that the temperature-induced residual stresses are not a problem of crack formation but of crack propagation. Cracks are not formed but already existing haircracks are spread and enlarged. An increasing bending strength can, therefore, certainly not lead to an increased resistance to crack formation.

Large Anodes

The biggest anode produced by ALUCHEMIE has the dimensions 1430\*1000 mm, height 560 mm. The results of this calculation can be seen from Fig. 4. If one compares the results with those of Fig. 2 (small anode), the following important statement has to be made:

The general anode size, i.e. the geometrical factors length, width and height, have no influence on the size of the residual stresses. Thermal shock cracks will occur very similarly on large and small anodes at the bottom corners.

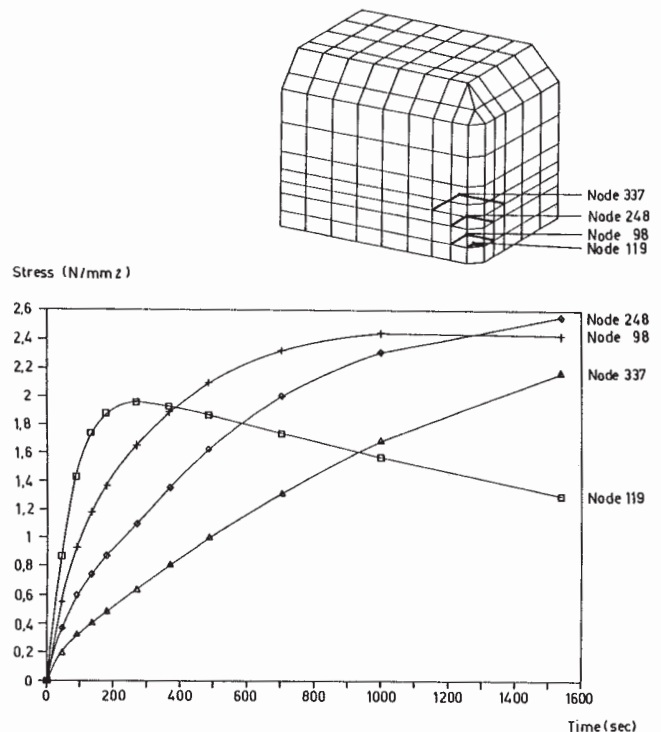


Fig. 4: Stresses as function of the time at different nodes of a large anode

Different Immersion Depths

When a new anode is set at a specific inter-polar distance, different immersion depths of the anode result as the electrolyte height fluctuates. In order to examine such effects, besides the standard immersion depth of 15 cm, depths of 11 and 19 cm were also chosen. The corresponding results are entered in Fig. 5. For the correlations, dimensionless factors were chosen: The respective immersion depth is divided by its standard value (15 cm) and the maximum residual stress by the value in the standard type.

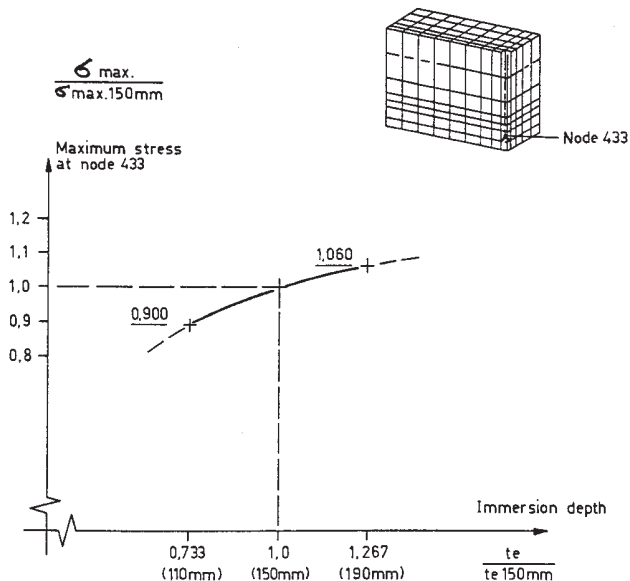


Fig. 5: The maximum forced stresses as function of the immersion depth of the anodes

The curve shows that there is a correlation between immersion depth and residual stress but that it is not very marked; the curve is relatively flat. Particularly for greater immersion depths it can be read that the dependence declines. It is to be suspected that this factor is moving towards a limit value for high immersion depths.

If on the other hand one goes from the standard value 15 cm down, then the curve seems to become more and more steep i.e. the dependence between maximum stress and immersion depth becomes more and more marked. The curve, however, does not go through the origin of the coordinates. Even at immersion depth zero, when the anode just touches the electrolyte, stresses already develop.

In practice, the depth of the electrolyte can vary considerably; for example extreme values between 15 and 35 cm were found. It can be estimated from Fig. 5 that even at extreme immersion depths, only an increase in the maximum residual stress of 10 - 13 % can take place. This should not lead to a significant increase in cracked anodes.

Influence of the Thermal Expansion Coefficient

In order to study the influence of the thermal expansion coefficient, the calculations were repeated with the following values:

$$\alpha = 2.625 \cdot 10^{-6}$$

$$\alpha = 5.000 \cdot 10^{-6}$$

and compared with the standard value

$$\alpha = 3.500 \cdot 10^{-6} \text{ (results in Fig. 2).}$$

The stresses resulting from the changed expansion coefficients can be seen from Figs. 6 and 7.

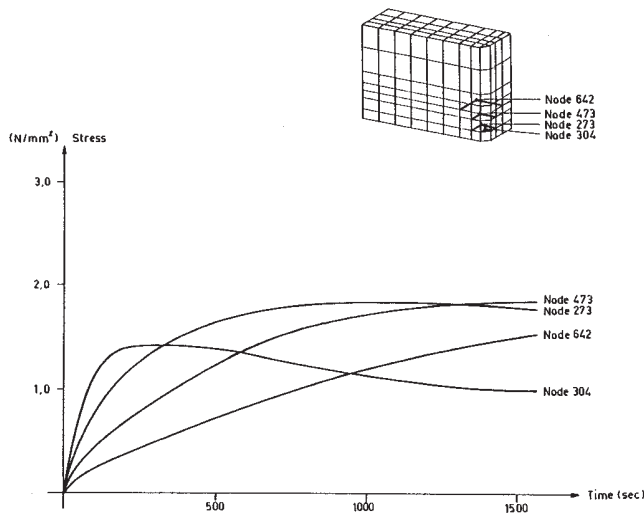


Fig. 6: Stress curves as function of the time in different nodes at  $\alpha = 2.625 \cdot 10^{-6} \text{ 1/K}$

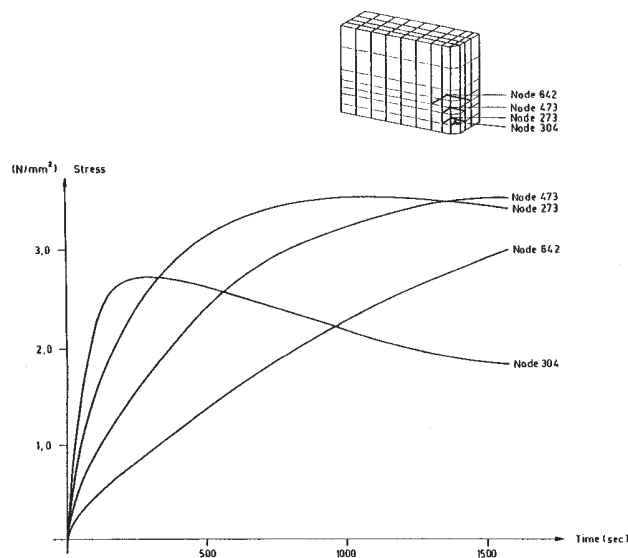


Fig. 7: Stress curves of different nodes as function of the time with  $\alpha = 5.0 \cdot 10^{-6} \text{ 1/K}$

If all the results are compared, it is found that the thermal expansion coefficient and the residual stresses are strictly proportional. If the value  $\alpha$  increases by 20 %, then the stresses also become 20 % greater.  $\alpha$  is, therefore, a very important factor for the crack resistance of the anodes.

In the above calculation it was presumed of course that besides  $\alpha$  no other material property is changed and therefore  $\bar{\alpha}$  is also not coupled with other material properties.

It remains to be recorded that  $\alpha$  is an extremely important factor for the quality of the anodes. Since a direct connection has been observed between  $\alpha$  on the one hand and the kind of coke on the other, an important assessment criterion is obtained for the qualification of the different kinds of coke. In particular also indications for the blending ratio for different types of coke result.

Influence of Young's Modulus

Three cases are again examined:

$E = 9514 \text{ N/mm}^2$   
 $E = 5437 \text{ N/mm}^2$

and compared with the standard value

$E = 6796 \text{ N/mm}^2$ .

According to the available results, it suffices to compare the stresses in the bottom corners in critical nodes.

One obtains:

E	$\sigma$
N/mm <sup>2</sup>	N/mm <sup>2</sup>
5437	1.53
6796	1.91
9514	2.67

Table 2: Dependence of residual stresses on different values of Young's modulus

This shows that E and the corresponding residual stresses are directly proportional. For every random value of E the resulting residual stress can be calculated very simply by hand.

After a very marked dependence of the tensions on the temperature expansion coefficient was ascertained, the same result is obtained in the case of E. Every alteration of E goes over to the residual stresses in the same degree.

Influence of the Thermal Conductivity

Here too three cases were examined:

$\lambda = 2.325 \text{ W/mK}$   
 $\lambda = 4.65 \text{ W/mK}$

and compared with the value

$\lambda = 3.1 \text{ W/mK}$ .

The results are entered in Diagram 8. The figures are given relative to those of the standard case.

Now that both for the thermal expansion and for Young's modulus a direct proportionality was ascertained, an entirely different relation results in the case of the thermal conductivity. With greater

$\lambda$  the maximum stresses become smaller; furthermore the correlation, as Fig. 8 shows, is not linear. A consideration of extreme values shows that the residual stresses must disappear if  $\lambda$  becomes very large. Vice versa the residual stresses become infinitely great, when  $\lambda$  goes towards zero. The curve has, therefore, a hyperbolic function which approaches the two coordinate axes asymptotically.

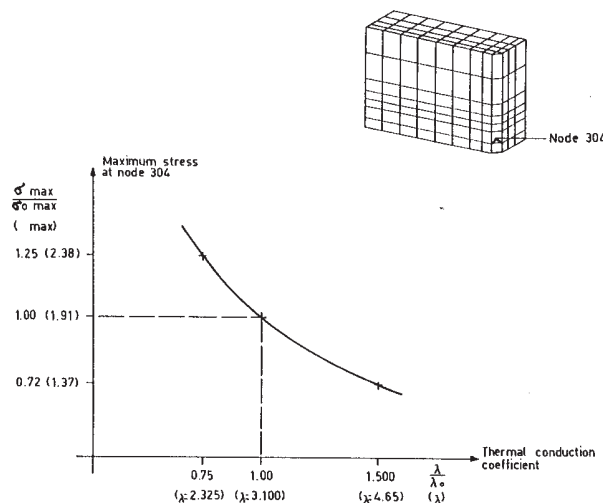


Fig. 8: Relation between maximum stress in nodes 304 and the thermal conductivity

It is to be mentioned that with variable  $\lambda$ , the temperatures on the contact surfaces to the electrolyte also change. Since in the initial phase after setting probably a thin crust of flux forms on the anode, this crust could also be influenced by  $\lambda$ . If  $\lambda$  is small, the outside temperature on the anode rises and possibly as a result also the crusts become thinner, which reinforces the heat supply. As a result the temperature gradients also become a bit larger. Since this calculation is based on a constant heat transfer coefficient flux - anode, probably the dependence between  $\lambda$  and the maximum residual stress is somewhat underestimated.

Influence of the Anodic Current

In a variation to the standard case it is assumed that the anode current will reach a current, again in 18 hours, which is 30 % above the anode nominal current.

The temperature calculations already show that the variant with higher current does not differ from the standard case. The heating capacity of the current in the first 25 minutes amounts to only a few percent of the nominal current heating power. Differences in this heating power are, therefore, unimportant; effects on the mechanical stresses do not have to be calculated, therefore.

Influence of the Electrolyte Temperature

The electrolyte temperature can at most be too high for an anode. That is why, besides the standard temperature of

$T = 9650 \text{ C}$

two other temperatures

- T = 985 °C (slightly sick pot)
- T = 1050 °C (very sick pot or situation after longer anode effect)

were taken into account. The results are summarized in Fig. 9:

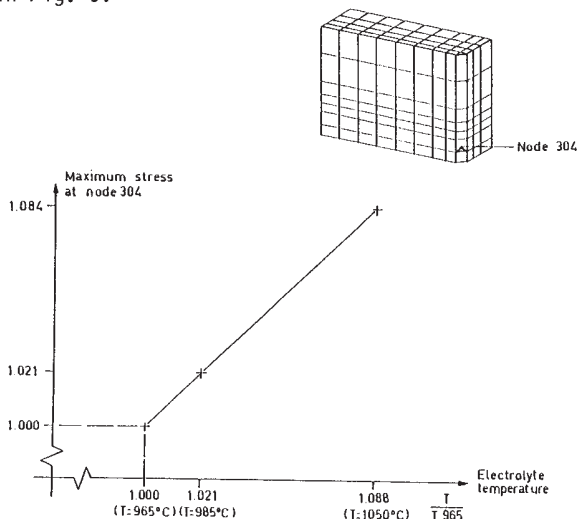


Fig. 9: Correlation between electrolyte temperature and resulting residual stresses

The curve in Fig. 9 is slightly bent; it flattens off a bit with rising flux temperatures. In the range of the temperatures which occur in practice, the stress variation tends to be small and is about 8 % max.

Nevertheless caution is called for. Small heat transfer coefficients between flux and anode can only be explained with a crust. The calculations were now all carried out with the same coefficient. A higher flux temperature could possibly influence this crust, which of course would also change the heat transfer coefficient. This dependence of the stresses on the flux temperature is possibly underestimated, therefore.

Summarising Assessment  
Influence of Parameters

To put it very summarily, the analysis of the variation of the parameters thermal expansion, Young's modulus, thermal conductivity, anodic current and electrolyte temperature has supplied the following influences on the maximum residual stresses

- variation of  $\alpha$ : the thermal expansion and the maximum stress are exactly proportional
- variation of E: also the Young's modulus shows a strict proportionality to the resulting stress
- variation of  $\lambda$ : the heat conductivity has a hyperbolic dependence to the stress; the greater  $\lambda$  becomes, the smaller  $\sigma$  becomes.

- variation of I: the anodic current has, within the range of the computation accuracy no influence on the extent of the stresses
- variation of T: approximate proportionality between flux temperature and stresses
- variation of the immersion depth: the stresses increase slightly with increasing immersion depth.

For the anode producer, however, anodic current, electrolyte temperature, depth of electrolyte and immersion depth cannot be influenced. These factors should not be taken into account in the quality figure  $Q_T$ s, therefore, since they do not represent any anode property.

The above results confirm the structure of the quality figure  $Q_s$  completely.

If the dependency of the stresses of  $\alpha$ , E and  $\lambda$  are linearized, the following approximation equations result:

- for  $\alpha$ :  $\sigma/\sigma_0 = 1 + 1.000 \cdot (\alpha/\alpha_0 - 1)$
- for E:  $\sigma/\sigma_0 = 1 + 1.000 \cdot (E/E_0 - 1)$
- for  $\lambda$ :  $\sigma/\sigma_0 = 1 - 0.705 (\lambda/\lambda_0 - 1)$

These relations also confirm the abovementioned defined quality figure in their main elements.

With that both with the method of calculation described and also with the quality figure, a good possibility is available for forecasting and changing the thermal shock behaviour of anodes.

Bibliography:

- 1 D. P. Hasselmann: "Unified Theory of Thermal Shock Fracture Initiation and Crack Propagation in Brittle Ceramics", Journal of The American Ceramic Society, (1969), 600 - 604
- 2 W. D. Kingery, Introduction to Ceramics, 2nd Ed., Wiley (1976), New York "Thermal and Compositional Stresses", 816 ff
- 3 J. A. Brown, P. J. Rhedey: "Characterization of Prebaked Anode Carbon by Mechanical and Thermal Properties", Light Metals 1975, 253 - 269
- 4 J. Nakayama, M. Ishizuka: "Experimental Evidence for Thermal Shock Damage Resistance", American Ceramic Society Bulletin, Vol. 45, No. 7, (1966), 666 - 669
- 5 W. Schmidt-Hatting, A. A. Kooijman, P. Van den Bogerd: "Sensitivity of Anodes for the Electrolytic Aluminium Production to Thermal Shocks", Light Metals 1988, 253 - 257
- 6 T. Log, H. A. Oye: "Thermal Conductivity of Prebaked Anodes", Aluminium, 65. Jahrgang 1989, Heft 5, 508 - 511
- 7 TPS10-Bedienungshandbuch, T-Programm GmbH, Reutlingen (BRD), 1984